Journal of
Medicinal
Chemistry

Volume 41, Number 19 September 10, 1998

Communications to the Editor

(*Z*,*Z*)-2,7-Bis(4-amidinobenzylidene)cycloheptan-1-one: Identification of a Highly Active Inhibitor of Blood Coagulation Factor Xa

Kenneth J. Shaw,* William J. Guilford, Jerry L. Dallas, Sunil K. Koovakkaat, Margaret A. McCarrick, Amy Liang, David R. Light, and Michael M. Morrissey

Discovery Research, Berlex Biosciences, 15049 San Pablo Avenue, P.O. Box 4099, Richmond, California 94804-0099

Received May 5, 1998

Factor Xa (FXa) is a trypsin-like serine protease that plays a key role in the blood coagulation cascade. It holds a central position that links the intrinsic and extrinsic pathways to the final common pathway of coagulation. Classically, the primary role of FXa is the proteolytic activation of thrombin, after combining with factor Va and calcium on a phospholipid membrane to form the prothrombinase complex.[1] Thrombin, in turn, promotes blood clot formation by catalyzing the formation of polymerizable fibrin from fibrinogen in addition to activating platelets. Free FXa, unbound to factor Va, triggers coagulation via the direct activation of factors V and IX[2] and binds to effector cell protease receptor-1 on platelets, augmenting membrane assembly of prothrombinase.[3] Ex vivo data demonstrates that prothrombinase, not thrombin, is the major determinant of the procoagulant activity of human whole-blood clots.[4]

The oral anticoagulant, warfarin,[5] and the parenteral anticoagulant, heparin,[6] are used extensively in the clinic. The slow onset of action and requirement to monitor warfarin generated interest in direct acting anticoagulants, such as inhibitors of thrombin.[7] Although not orally available, hirudin is a highly selective, direct acting proteinaceous inhibitor of thrombin. Hirudin has been tested in the clinic and is efficacious but does not show improvement in bleeding tendency when compared to heparin.[8] The proteinaceous FXa inhibitors, antistasin and tick anticoagulant peptide (TAP), have been tested in a wide variety of preclinical models of venous and arterial thrombosis.[9] A direct comparison of TAP with the proteinaceous thrombin inhibitor, hirudin, demonstrated that under conditions of equivalent efficacy a greater bleeding tendency was observed with hirudin.[10] Results with these parenterally administered anticoagulants in preclinical efficacy models suggest that a selective inhibitor of FXa will be efficacious and may have a superior therapeutic ratio compared to an inhibitor of thrombin. By initiating a program which targets orally available inhibitors of FXa, we hoped to develop a direct acting anticoagulant with a good therapeutic window.

There are several examples of bisamidine compounds that have been shown to be inhibitors of FXa.[11] Stürzebecher et al. have reported a series of conformationally restricted bisamidine inhibitors with the most potent inhibitor, 2,7-bis(4-amidinobenzylidene)cycloheptan-1-one (BABCH, **1a**), exhibiting a K_i value of 13 nM for bovine FXa.[12,13] At the initiation of our program, we decided to utilize **1a** as a standard to validate our primary enzyme and anticoagulant assays. BABCH (**1a**) was prepared as previously described[14] by condensation of 4-amidinobenzaldehyde hydrochloride with cycloheptanone in 85% phosphoric acid at 100 °C (Scheme 1). A crystalline solid (purity >99% by HPLC and ^{1}H NMR, mp >360 °C) was obtained with spectral data identical with the literature report. The ^{1}H NMR and ^{13}C NMR spectra are consistent with a symmetrical configuration, since the vinyl protons appear as a singlet integrating for two protons, and the ^{13}C NMR spectra show only 10 unique carbon atoms (Table 1). The downfield chemical shift of the vinylic protons ($\delta = 7.33$ ppm) is consistent with other reported α,β-unsaturated cyclic ketones having (*E*,*E*) double bond configurations.[15,16] Further confirmation of the (*E*,*E*) orientation of the exocyclic double bonds was obtained from NOESY NMR studies (Table 1). In these studies, a positive NOE was observed between the cycloheptanone ring protons (C-3 and C-4 positions, Table 1) and the C-7 aromatic protons with no observed NOE between the vinylic protons (C-5 position) and the cycloheptanone protons.

Compound **1a** displayed considerable variability when initially evaluated in our FXa chromogenic assay (K_i

S0022-2623(98)00281-7 CCC: $15.00
Published on Web 08/15/1998

Scheme 1

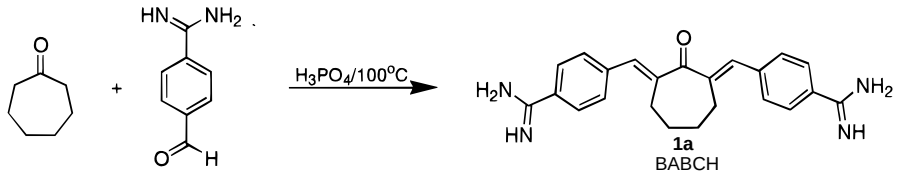

Table 1. ^{1}H, ^{13}C, and NOESY Data of Olefin Isomers **1a**−**3a**[a]

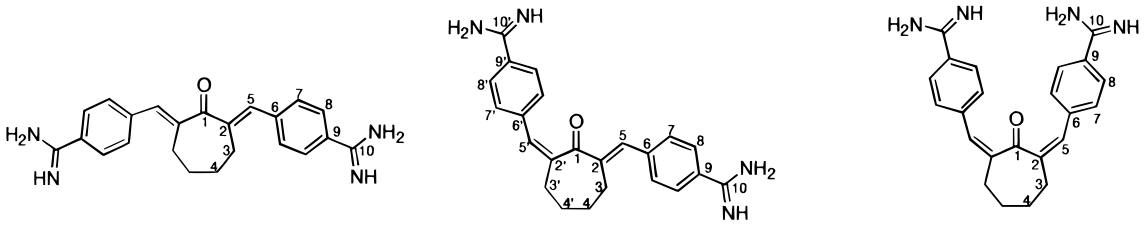

	(*E*,*E*) isomer (**1a**)			(*E*,*Z*) isomer (**2a**)			(*Z*,*Z*) isomer (**3a**)		
carbon	^{13}C[b]	^{1}H[c]	NOESY[d]	^{13}C	^{1}H	NOESY	^{13}C	^{1}H	NOESY
1	197.37			198.76			197.91		
2	140.56			140.22			141.61		
3	27.44	2.66(m)	H7	27.21	2.71(m)	H7	35.40	2.56(m)	H5
4	27.86	1.90(m)	H7	29.28	1.89(m)	H7	31.79	1.89(m)	
5	133.36	7.33(s)	H7	134.74	7.60(s)	H7	134.36	6.94(s)	H3,7
6	143.71			141.17			144.60		
7	129.64	7.70(d)	H3,4,5	129.78	7.69(d)	H3,4,5	128.80	7.44(d)	H5
8	128.46	7.93(d)		128.45	7.89(d)		127.71	7.70(d)	
9	127.40			128.05			126.89		
10	165.14			165.16			165.20		
2′				140.83					
3′				35.13	2.47(m)	H5′			
4′				31.70	1.89(m)				
5′				129.69	6.79(s)	H3′,7′			
6′				147.77					
7′				128.47	7.40(d)	H5′			
8′				128.27	7.74(d)				
9′				126.80					
10′				165.20					

[a] All samples employed 9 mg quantities of solute in 0.5 mL of DMSO-d_6 on a Varian UP 400 spectrometer. Samples were protected from light sources. [b] Carbon-13 assignments are based on 2D heteronuclear correlation spectra; HETCOR (ref 30), FLOCK (ref 31), HMQC (ref 32), and HMBC (ref 33). [c] NMR chemical shifts are reported in ppm (δ) downfield from tetramethylsilane using internal DMSO-d_6 (^{1}H = 2.49 ppm, ^{13}C = 39.5 ppm); NH resonances are omitted. [d] 2D NOESY experiments were run in accordance with ref 34.

values ranged between 16 and 260 nM). Since α,β-unsaturated ketones are known to undergo a variety of photorearrangements,[17] we postulated that the inconsistent K_i values obtained for **1a** could be a result of photochemical isomerization prior to binding with FXa. This hypothesis is supported by a report by Aizenshtat et al.[16] describing the photoisomerization of the unsubstituted (*E*,*E*)-2,7-benzylidene-cycloheptan-1-one (**1b**) to a mixture of the (*E*,*Z*) and (*Z*,*Z*)-isomers (**2b** and **3b**, respectively, Scheme 2). Therefore, to fully characterize the BABCH system, we investigated the photochemically induced isomerization of **1a**. The results are described below and clearly illustrate that the most active FXa inhibitor of the BABCH series is the (*Z*,*Z*) isomer (**3a**).

Irradiation of an aqueous acetonitrile solution of **1a** with a 450 W high-pressure mercury lamp produced two new compounds as determined by HPLC. The new compounds were separated by reverse-phase HPLC and identified as the (*E*,*Z*) and (*Z*,*Z*) isomers (**2a** and **3a**, respectively).[18,19] The photoisomerization produces an equilibrium mixture of 55% **2a**, 40% **3a**, and <5% **1a** (by ^{1}H NMR analysis), similar to the isomer distribution reported for the photoisomerization of **1b**.[16] Irradiation of an aqueous methanolic solution of the meta analogue (**1c**) produced comparable results. The three isomeric para bisamidine cycloheptanones (**1a**, **2a** and **3a**) could be differentiated and unambiguously assigned from their characteristic NMR spectra (Table 1). The ^{13}C NMR of **2a** shows 19 unique carbon atoms, and the ^{1}H NMR shows separate resonances for many of the protons. These data clearly illustrate that **2a** is asymmetric, and therefore only the (*E*,*Z*) configuration is consistent with these data. The ^{1}H NMR and ^{13}C NMR spectra of **3a** show the same elements of symmetry as **1a**: the two vinylic protons appear as a singlet integrating for two protons, and the ^{13}C NMR shows 10 unique carbon atoms. The upfield chemical shift of the vinylic protons (δ = 6.94 ppm) is consistent with related compounds containing the same double bond configuration,[16] and a positive NOE between the vinylic and allylic protons unambiguously supports this structure (Table 1).

The bisamidine isomers were evaluated for their FXa inhibitory activities in the absence of light.[20] The results in Table **2** clearly demonstrate that **3a** is the most potent FXa inhibitor (K_i = 0.66 nM)[21] in the BABCH series, while **2a** also exhibits significant FXa

Scheme 2

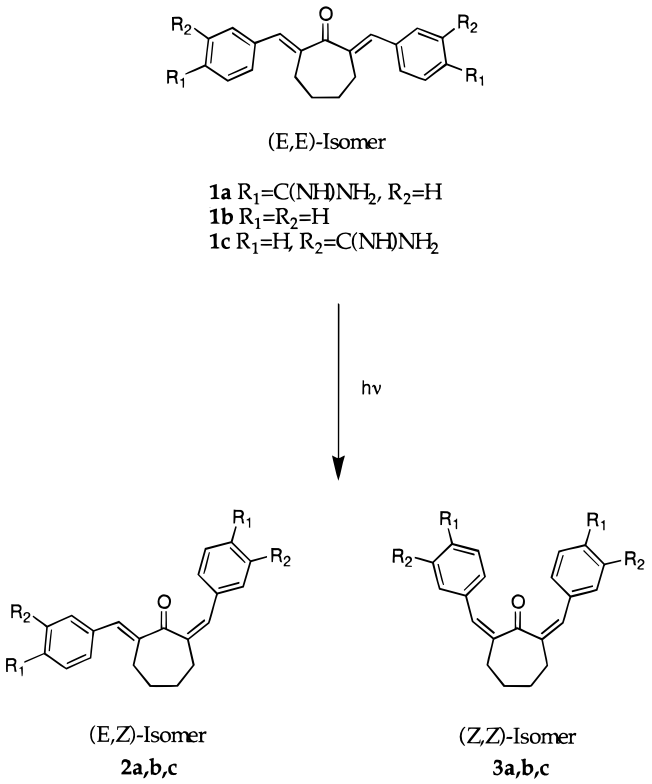

Table 2. In Vitro Inhibitory Activities of Bisamidine Isomers against Factor Xa (Human), Thrombin (Human), and Trypsin (Bovine) Tested in the Absence of Light

	K_i (nM)[a]		
compd[b]	factor Xa	thrombin	trypsin
1a	17000	6200	280
2a	200	130	29
3a	0.66	530	33
1c	1400	2100	410
2c	140	1000	200
3c	5.6	1400	44

[a] K_i values for these competitive inhibitors are averaged from multiple determinations ($n > 2$) and the standard deviations are <30% of the mean.[21] [b] All compounds gave satisfactory analytical data (C, H, N; ±0.4% of theoretical values).

inhibitory activity (K_i = 200 nM). As can be seen in Table 2, **3a** also showed selectivity against the related serine proteases, thrombin and trypsin. Interestingly, when **1a** was tested in the absence of light we found very low FXa inhibitory activity (K_i = 17 μM). Thus, the K_i value of 13 nM obtained in the original study[13] can be attributed to the presence of isomers **2a** and **3a** in the sample resulting from photochemical isomerization. In our hands, the measured FXa inhibitory activity of **1a** was variable when measured in the presence of light and could be correlated with the extent of isomerization. Similar results were seen with the 6, 8, 9, and 10 membered cycloalkanones.[18] The meta series (**1c**−**3c**) showed a similar order of inhibitory potency for the three isomers; however the (*E*,*E*) isomer (**1c**) is clearly more potent and the (*Z*,*Z*) isomer (**3c**) significantly less potent than their corresponding para isomers.

Molecular modeling studies of the three para isomers (**1a**−**3a**) bound to FXa were carried out to provide an understanding of the structure−activity relationships

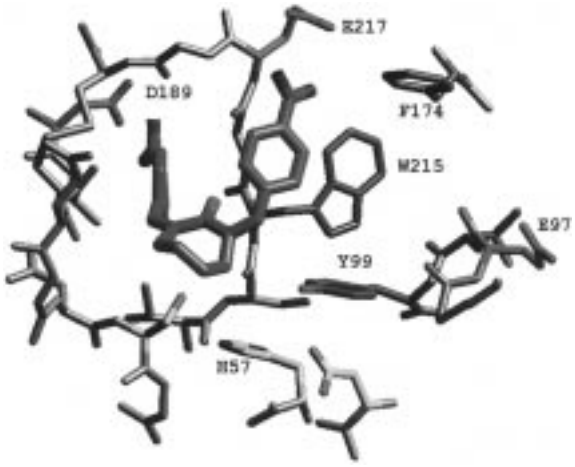

Figure 1. Proposed U-shaped binding mode of **3a** (green) within the FXa active site.

for these three inhibitors.[22] The structure of the catalytic domain used for these modeling studies came from FXa crystallographic coordinates.[23] An important feature common to benzamidine-based serine protease inhibitors is salt-bridge formation between the highly basic amidine group and Asp-189 in the S1 pocket.[24] Using this interaction as an anchoring site, the para bisamidine isomers (**1a**−**3a**) were docked into the active site with one of the benzamidine groups bound to Asp-189, and the remaining portion of each molecule was oriented to allow for potentially favorable interactions with the enzyme. Analysis of the possible binding modes of the (*E*,*E*) isomer (**1a**) suggests that the second benzamidine group is solvent exposed, explaining the relatively poor inhibitory potency of this isomer. The (*Z*,*Z*) isomer (**3a**) can potentially bind to FXa by forming two salt bridges. One of the benzamidine groups can interact with Asp-189 in the S1 pocket, while the second amidine can interact with Glu-217 (Figure 1). Formation of a second salt bridge with Glu-217 could contribute significantly to the affinity of **3a** for FXa and helps to explain its potency relative to **1a** and **2a**. The (*E*,*Z*) isomer (**2a**) may bind in an orientation similar to the published X-ray structures of the low molecular weight FXa inhibitor, DX-9065a.[25] This inhibitor was docked into the active site with the benzamidine group coming off of the (*Z*) olefin bound into the S1 pocket, in a manner consistent with **1a**. In this extended conformation, the second benzamidine group (attached to the (*E*) olefin) can bind in the S4 subsite[26] formed by the aromatic residues Tyr-99, Phe-174, and Trp-215 (Figure 2). This subsite is lined by carbonyl groups which can accommodate the positive charge of a basic group as was noted by Brandstetter et al.[25] In this binding mode, the second amidine group of **2a** can be positioned to interact with the peptide backbone carbonyl groups of Lys-96, Glu-97, and Thr-98.

Molecular dynamics (MD) studies were performed to investigate the stability of **3a** in the postulated U-shaped conformation.[27] Two different results were found depending upon the initial restraints used. In the first experiment, the U-shaped conformation of **3a** was bound in the FXa active site with salt bridges to Asp-189 and Glu-217 as described above. Harmonic restraints were used to prevent the two salt bridges from breaking for the first 100 ps of dynamics. These

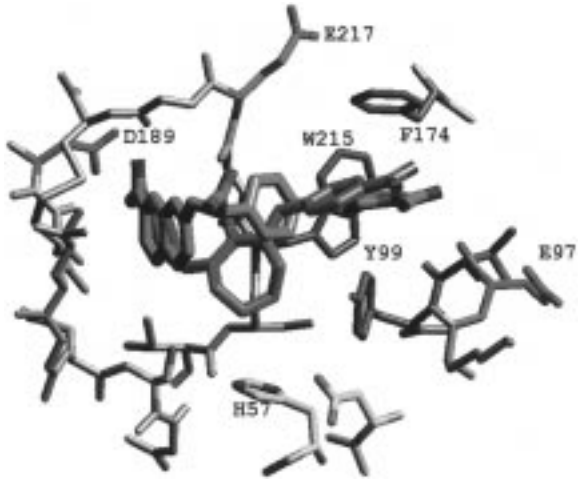

Figure 2. Proposed binding mode of extended conformation of **2a** (green) and X-ray coordinates of DX-9065a (pink) within the FXa active site.

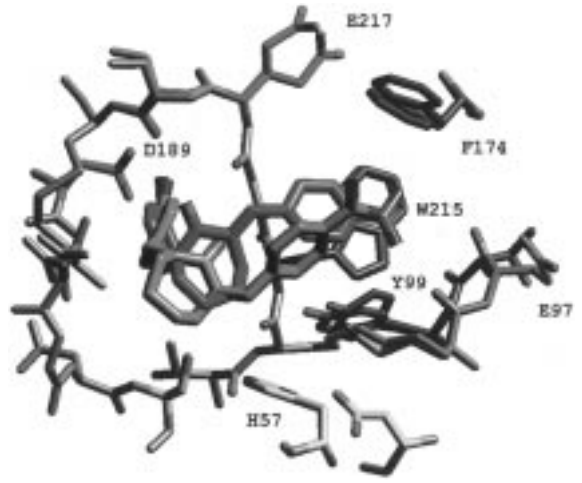

Figure 3. Overlay of extended structures derived from molecular dynamics calculations of **2a** (green) and **3a** (pink) within the FXa active site. (Structures have been minimized after dynamics calculations.)

restraints were removed and the MD simulation was continued for over 1 nanosecond. Under these conditions, the U-shaped conformation remained bound to Glu-217 for up to 800 ps, indicating that this mode of binding is relatively stable. In the second experiment, the same initial geometry of **3a** complexed to FXa was used, but only the salt bridge to Asp-189 was restrained during the first 100 ps. Surprisingly, within 10 ps **3a** adopted an extended conformation rather than forming a salt bridge with Glu-217. This extended conformation allows **3a** to bind to FXa in a fashion similar to the proposed binding mode of **2a** (Figure 3), making contacts between the unrestrained benzamidine group and the carbonyl groups of Lys-96, Glu-97, and Thr-98.[28] In this binding mode, additional hydrophobic contacts are made with Gln-192, Tyr-99, and Trp-215. The same molecular dynamics procedure was repeated with **2a**, which showed a strong tendency to remain bound in the extended mode (Figure 3). Should subsequent studies show that both **3a** and **2a** bind in the extended conformation suggested by these molecular dynamics calculations, the observed 300-fold difference in potency between these isomers would be difficult to rationalize by inspection of molecular models alone. While these molecular dynamics calculations provide some initial suggestions to the conformations attained by these inhibitors upon binding to FXa, further inferences await the crystal structure of these isomers complexed with FXa.

In conclusion, experimental evidence is provided to support the assignment of **3a** as the bioactive olefin isomer in the BABCH series. This isomer is a potent sub-nanomolar inhibitor, more than 20 000 times more active than **1a**, and shows approximately 800-fold selectivity for FXa versus thrombin. Molecular modeling suggests two possible binding conformations, one of which is a unique U-shaped conformation which forms salt bridges to both Asp-189 and Glu-217. Although weaker than **3a**, the inhibitor **2a** also shows good FXa potency and is suggested to have a mode of binding similar to that observed for other reversible low molecular weight FXa inhibitors.[25a,29] Several analogous (*E*,*Z*) and (*Z*,*Z*) bis- and monoamidine analogues have been prepared by photoisomerization of the corresponding (*E*,*E*) isomers[18] and will be detailed in a future publication. These conformationally restricted inhibitors have proved to be a useful template for the design of distinct classes of potent, selective, and orally active FXa inhibitors. Progress in this area will be reported in the following communication and in future publications.

Acknowledgment. We thank Drs. Les Browne, William Dole, John Morser, and Mark Sullivan for their support and encouragement of this effort.

Supporting Information Available: ^{1}H NMR and NOESY spectral data for **1a**−**c** and ^{1}H NMR spectral data for **3a**−**c** (9 pages). Ordering information is given on any current masthead page.

References

(1) Mann, K. G.; Nesheim, M. E.; Church, W. R.; Haley, P.; Krishnaswamy, S. Surface-dependent reactions of the vitamin K-dependent enzyme complexes. *Blood* **1990**, *76*, 1−16.

(2) Lawson, J. H.; Kalafatis, M. K.; Stram, S.; Mann, K. G. A model for the tissue factor pathway to thrombin. *J. Biol. Chem.* **1994**, *269*, 23357−23366.

(3) (a) Ambrosini, G.; Plescia, J.; Chu, K. C.; High, K. A.; Altieri, D. C. Activation-dependent exposure of the inter-EGF sequence Leu83-Leu88 in factor Xa mediates ligand binding to effector cell protease receptor-1. *J. Biol. Chem.* **1997**, *272*, 8340−8345. (b) Bouchard, B. A.; Catcher, C. S.; Thrash, B. R.; Adida, C.; Tracy, P. B. Effector cell protease receptor-1, a platelet activation-dependent membrane protein, regulates prothrombinase-catalyzed thrombin generation. *J. Biol. Chem.* **1997**, *272*, 9244−9251.

(4) Eisenberg, P. R.; Siegel, J. E.; Abendschein, D. R.; Miletich J. P. Importance of factor Xa in determining the procoagulant activity of whole-blood clots. *J. Clin. Invest.* **1993**, *91*, 1877−1883.

(5) (a) Hirsh, J. Oral anticoagulant drugs. *N. Engl. J. Med.* **1991**, *324*, 1865−1875. (b) Hirsh, J.; Fuster, V. Guide to anticoagulant therapy. Part 2: Oral anticoagulants. *Circulation* **1994**, *89*, 1469−1480.

(6) Hirsh, J.; Fuster, V. Guide to anticoagulant therapy. Part 1: Heparin. *Circulation* **1994**, *89*, 1449−1468.

(7) Lefkovits, J.; Topol, E. J. Direct thrombin inhibitors in cardiovascular medicine. *Circulation* **1994**, *90*, 1522−1536.

(8) (a) Antman, E. M. TIMI 9A investigators. Hirudin in acute myocardial infarction. Safety report from the thrombolysis and thrombin inhibition in myocardial infarction (TIMI) 9A trial. *Circulation* **1994**, *90*, 1624−1630. (b) GUSTO IIa investigators. Randomized trial of intravenous heparin versus recombinant hirudin for acute coronary syndromes. *Circulation* **1994**, *90*, 1631−1637. (c) Neuhaus, K.-L.; Essen, R. v.; Tebbe, U.; Jessel, A.; Heinrichs, H.; Mäurer, W.; Döring, W.; Harmjanz, D.; Kötter, V.; Kalhammer, E.; Simon, H.; Horacek, T. Safety observations from the pilot phase of the randomized r-hirudin for the improvement of thrombolysis (HIT-III) study. *Circulation* **1994**, *90*, 1638−1642.

(9) (a) Vlasuk, G. P. Structural and functional characterization of tick anticoagulant peptide (TAP): A potent and selective inhibitor of blood coagulation factor Xa. *Thrombosis Haemost.* **1993**, *70*, 212−216. (b) Vlasuk, G. P.; Ramjit, D.; Fujita, T.; Dunwiddie, C. T.; Nutt, E. M.; Smith, D. E.; Shebuski, R. J. Comparison of the in vivo anticoagulant properties of standard heparin and the highly selective factor Xa inhibitors antistasin and tick anticoagulant peptide (TAP) in a rabbit model of venous thrombosis. *Thrombosis Haemost.* **1991**, *65*, 257−262. (c) Mellott, M. J.; Holahan, M. A.; Lynch, J. J. Acceleration of recombinant tissue-type plasminogen activator-induced reperfusion and prevention of reocclusion by recombinant antistasin, a selective factor Xa inhibitor, in a canine model of femoral arterial thrombosis. *Circulation Res.* **1992**, *70*, 1152−1160.

(10) (a) Sitko, G. R.; Ramjit, D. R.; Stabilito, I. I.; Lehman, D.; Lynch, J. J.; Vlasuk, G. P. Conjunctive enhancement of enzymatic thrombolysis and prevention of thrombotic reocclusion with the selective factor Xa inhibitor, Tick Anticoagulant Peptide: comparison to hirudin and heparin in a canine model of acute coronary artery thrombosis. *Circulation* **1992**, *85*, 805−815. (b) Harker, L. A.; Hanson, S. R.; Kelly, A. B. Antithrombotic benefits and hemorrhagic risks of direct thrombin antagonists. *Thrombosis Haemost.* **1995**, *74*, 464−472.

(11) (a) Tidwell, R. R.; Webster, W. P.; Shaver, S. R.; Geratz, J. D. Strategies for anticoagulation with synthetic protease inhibitors. Xa inhibitors versus thrombin inhibitors. *Thrombosis Res.* **1980**, *19*, 339−349. (b) Nagahara, T.; Yukoyama, Y.; Inamura, K.; Kayakura, S.; Komoriya, S.; Yamaguchi, H.; Hara, T.; Iwamoto, M.; Dibasic(amidinoaryl)propanoic acid derivatives as novel blood coagulation factor Xa inhibitors. *J. Med. Chem.* **1994**, *37*, 1200−1207. (c) Quan, M. L.; Pruitt, J. R.; Ellis, C. D.; Liauw, A. Y.; Galemmo, R. A.; Stouten, P. F. W.; Wityak, J.; Knabb, R. M.; Thoolen, M. J.; Wong, P. C.; Wexler, R. R. Bisbenzamidine isoxazoline derivatives as factor Xa inhibitors. *Bioorg. Med. Chem. Lett.* **1997**, *7*, 2813−2818. (d) Sato, K.; Kawasaki, T.; Hisamichi, N.; Taniuchi, Y.; Hirayama, F.; Koshio, H.; Matsumoto, Y. Antithrombotic effects of YM-60828, a newly synthesized factor Xa inhibitor, in rat thrombosis models and its effects on bleeding time. *Br. J. Pharmacol.* **1998**, *123*, 92−96.

(12) Stürzebecher, J.; Markwardt, F.; Walsmann, P. Synthetic Inhibitors of Serine Proteinases XXIII. Inhibition of factor Xa by diamidines. *Thrombosis Res.* **1980**, *17*, 545−548.

(13) Stürzebecher, J.; Stürzebecher, U.; Vieweg, H.; Wagner, H.; Hauptmann, J.; Markwardt, F. Synthetic inhibitors of bovine factor Xa and thrombin. Comparison of their anticoagulant efficiency. *Thrombosis Res.* **1989**, *54*, 245−252.

(14) Wagner, G.; Vieweg, H.; Horn, H. Syntheses von α,α^1−bis-[amidinobenzyliden]- und α,α^1-bis-[amidinobenzyl]-cycloalkanonen. *Pharmazie* **1977**, *32*, 141−145.

(15) George, H.; Roth, H. J. Photoisomerisierung und cyclo-1,2-addition α,β−ungesättigter cyclanonen. *Tetrahedron Lett.* **1971**, *43*, 4057−4060.

(16) Aizenshtat, Z.; Hausmann, M.; Pickholtz, Y.; Tai, D.; Blum, J. Chlorocarbonylbis(triphenylphosphine)iridium-catalyzed isomerization, isoaromatization, and disproportionation of some cycloalkanones having exocyclic double bonds. *J. Org. Chem.* **1977**, *42*, 2386-2394.

(17) Margaretha, P. Photochemical rearrangement reactions in synthetic organic chemistry. In *Preparative Organic Photochemistry*; Lehn, J. M., Ed.; Springer-Verlag: New York, 1982; pp 31−33.

(18) (a) Dallas, J. L.; Guilford, W. J.; Koovakkat, S. K.; Morrissey, M. M.; Shaw, K. J. (Z,Z), (Z,E) and (E,Z) Isomers of substituted bis(phenylmethylene)cycloketones. U. S. Patent 5,633,381, 1997. (b) Guilford, W. J.; Shaw, K. J.; Dallas, J. L.; Koovakkat, S. K.; Liang, A.; Light, D.; Hinchman, J.; Post, J.; Morrissey, M. M. Design, synthesis, and biological activity of novel factor Xa inhibitors: 1. Z,Z-Substituted bis(amidinobenzylidene)cycloketone analogs. Presented at the 215th American Chemical Society National Meeting, March 29−April 2, 1998, Dallas, TX, Abstract 121.

(19) The photoisomerization of **1a** could also be effected with other light sources. Irradiation of an ethanolic solution of **1a** with a 150 W standard flood light for 3 days afforded the same equilibrium mixture of isomers (determined by ^{1}H NMR and HPLC). Purified samples of the (*E*,*Z*) and (*Z*,*Z*) isomers were also photochemically unstable in solution. Ethanolic solutions of both isomers, **2a** and **3a,** could be converted back to the equilibrium mixture, by irradiation with a 450 W high-pressure mercury lamp.

(20) Significant isomerization was also observed when a solution of **1a** was exposed to ambient light sources. After 3 days of standing on a laboratory benchtop, a DMSO solution of **1a** isomerized to a mixture containing 54% **2a**, 35% **3a**, and 11% **1a**. Solutions of **2a** and **3a** were similarly unstable to ambient light sources. Since solutions of these compounds were photochemically unstable, care was taken to exclude light during isolation and chemical or biochemical characterization studies.

(21) Commercial purified serine proteases, human factor Xa and thrombin (Enzyme Research Laboratories, Inc., South Bend, IN), and bovine cationic trypsin (Boehringer Mannheim, Corp., Indianapolis, IN) were assayed in 150 mM NaCl, 2.5 mM $CaCl_2$, 50 mM Tris-HCl, pH 7.5, and 0.1% PEG 6000 in a final assay volume of 200 μL at room temperature with Chromogenix substrates (Kabi Pharmacia Hepar, Inc., Franklin, OH). The final concentrations of enzyme and substrate were: Factor Xa (1 nM) and S-2222 (164 μM), thrombin (16 nM) and S-2302 (300 μM), and trypsin (16 nM) and S-2266 (127 μM). The inhibition mechanism is competitive, therefore a substrate concentration equal to K_m was used to assay varying concentrations of the inhibitor to determine the K_i. The K_i value of **3a** was determined by fitting data obtained at 0.3 and 1 nM FXa to a modification of the Morrison equation to correct for the proportion of inhibitor bound to the enzyme relative to free (Jordan, S. P.; Waxman, L.; Smith, D. E.; Vlasuk, G. P. Tick anticoagulant peptide: Kinetic analysis of the recombinant inhibitor with blood coagulation factor Xa. *Biochemistry* **1990**, *29*, 11095−11100. Morrison, J. F. Kinetics of the reversible inhibition of enzyme-catalysed reactions by tight-binding inhibitors. *Biochim. Biophys. Acta* **1969**, *185*, 269−286).

(22) Initial computational studies were carried out with the program BIOGRAF using the DREIDING force field: BIOGRAF Vers. 3.21, Molecular Simulations, Inc. Mayo, S. L.; Olafson, B. D.; Goddard, W. A. A generic force field for molecular simulations. *J. Phys. Chem.* **1990**, *94*, 8897−8909. The results of this analysis indicated that the potential amidine to amidine distances for **3a** (5−10 Å) are shorter than those for **2a** (11−13 Å). Subsequent studies using more accurate C═C bond parameters extended this distance in **3a** up to 12 Å.

(23) Padmanabhan, K.; Padmanabhan, K. P.; Tulinsky, A.; Park, C. H.; Bode, W.; Huber, R.; Blankenship, D. T.; Cardin, A. D.; Kisiel, W. Structure of human des(1−45) human factor Xa at 2.2Å resolution. *J. Mol. Biol.* **1993**, *232*, 947−966.

(24) (a) Bode, W.; Schwager, P. The refined crystal structure of bovine beta-trypsin at 1.8 Å resolution. II. Crystallographic refinement, calcium binding site, benzamidine binding site and active site at pH 7.0. *J. Mol. Biol.* **1975**, *98*, 693−717. (b) Marquart, M.; Walter, J.; Deisenhofer, J.; Bode, W.; Huber, R. The geometry of the active site and of the peptide groups in trypsin, trypsinogen and its complexes with inhibitors. *Acta Crystallogr.* Sect. B. **1983**, *39*, 480−490. (c) Banner, D. W.; Hadvary, P. Crystallographic analysis at 3.0 Å − Resolution of the binding to human thrombin of four active site-directed inhibitors. *J. Biol. Chem.* **1991**, *266*, 20085−20091.

(25) (a) Brandstetter, H.; Kühne, A.; Bode, W.; Huber, R.; Von Der Saal, W.; Wirhtensohn, K.; Engh, R. A. X-ray structure of active site-inhibited clotting factor Xa. *J. Biol. Chem.* **1996**, *271*, 29988−29992. (b) Stubbs, M. T.; Huber, R.; Bode, W. Crystal structures of factor Xa specific inhibitors in complex with trypsin: structural grounds for inhibition of factor Xa and selectivity against thrombin. *FEBS Lett.* **1995**, *375*, 103−107.

(26) The S4 or aryl-binding site is a continuation of an apolar binding subsite starting at S2. Rezaie, A. R. Role of Leu99 of Thrombin in Determining the P2 Specificity of Serpins. *Biochemistry* **1997**, *36*, 7437−7446.

(27) Molecular dynamics calculations were performed with AMBER: (a) Pearlman, D. A.; Case, D. A.; Caldwell, J. W.; Ross, W. S.; Cheatham III, T. E.; Ferguson, D. M.; Seibel, G. L.; Singh, U. C.; Weiner, P. K.; Kollman, P. A. AMBER 4.1, University of California, San Francisco, 1995, using published force field values: (b) Cornell, W. D.; Cieplak, P.; Bayly, C. I.; Gould, I. R.; Merz, K. M., Jr.; Ferguson, D. M.; Spellmeyer, D. C.; Fox, T.; Caldwell, J. W.; Kollman, P. A. A second generation force field for the simulation of proteins, nucleic acids, and organic molecules. *J. Am. Chem. Soc.* **1995**, *117*, 5179−5197. In addition to the standard parameter set, a new atom type and associated parameters were developed to describe olefin carbon atoms. Olefin geometries obtained with these parameters reproduce semiempirical (AM1) minimized geometries to within 0.02 Å for bond lengths and 2° for bond angles. AM1 minimizations were carried out using the MOPAC program provided in the Cerius^2 molecular modeling package, Molecular Simulations, Inc. (c) Stewart, J. J. P. MOPAC: A general molecular orbital package (Version 6.0), Frank J. Seiler Research Laboratory, U.S. Air Force Academy, Colorado Springs, CO 80840. (d) Dewar, M. J. S.; Zoebisch, E. G.; Healy, E. F.; Stewart, J. J. P. AM1: A new general purpose quantum mechanical molecular model. *J. Am. Chem. Soc.* **1985**, *107*, 3902−3909.

(28) Typical N to O distances between the amidine nitrogens of **3a** and oxygens of residues 96−99 are (residue, N1 distance, N2 distance in Å): Lys 96(C═O), 5.2−5.4, 5.8−6.1; Glu-97(C═O), 4.4−4.5, 5.6−5.9; Thr 98(C═O), 5.4−5.9, 7.6−8.1. Examination of the molecular dynamics structures shows that all these interactions are water-mediated.

(29) (a) Klein, S. I.; Czekaj, M.; Gardner, C. J.; Guertin, K. R.; Cheney, D. L.; Spada, A. P.; Bolton, S. A.; Brown, K.; Colussi, D.; Heran, C. L.; Morgan, S. R.; Leadley, R. J.; Dunwiddie, C. T.; Perrone, M. H.; Chu, V. Identification and initial structure−activity relationships of a novel class of nonpeptide inhibitors of blood coagulation factor Xa. *J. Med. Chem*. **1998**, *41*, 437−450. (b) Maduskuie, T. P.; McNamara, K. J.; Ru, Y.; Knabb, R. M.; Stouten, R. W. Rational design and synthesis of novel, potent bis-phenylamidine carboxylate factor Xa Inhibitors. *J. Med. Chem*. **1998**, *41*, 53−62.

(30) Bax, A.; Morris, G. A. An improved method for heteronuclear chemical shift correlation by two-dimensional NMR. *J. Magn. Reson*. **1981**, *42*, 501−505.

(31) Reynolds, W. F.; McLean, S.; Perpick-Dumont, M.; Enriquez, R. G. Improved carbon-13-proton shift correlation spectra for indirectly bonded carbons and hydrogens: the FLOCK experiment. *Magn. Reson. Chem*. **1989**, *27*, 162−169.

(32) Muller, L. Sensitivity enhanced detection of weak nuclei using heteronuclear multiple quantum coherence. *J. Am. Chem. Soc.* **1979**, *101*, 4481−4484.

(33) Bax, A.; Marion, D. Improved resolution and sensitivity in proton-detected heteronuclear multiple-bond correlation spectroscopy. *J. Magn. Reson*. **1988**, *78*, 186−191.

(34) Jeener, J.; Meir, B. H.; Bachmann, P.; Ernst, R. R. Investigation of exchange processes by two-dimensional NMR. *J. Chem. Phys.* **1979**, *71*, 4546−4553.

JM980281+